

# Potential of Agricultural Residue-Derived Biochar as a Salt-Adsorbent Amendment for Salinity Mitigation of Brackish Water for Irrigation

B. Thanh Nguyen<sup>1</sup>, G. Dai Dinh<sup>1</sup>, T. Xuan Nguyen<sup>1</sup>, D. Doan Do<sup>1</sup>, D. Thuy Phuc Nguyen<sup>1</sup>, A. Hung Le<sup>1</sup>, T. Ngoc Vu<sup>2</sup>, H. Thu Thi Tran<sup>3</sup>, N. Van Thai<sup>4\*</sup>, and Q. Van Luu<sup>5</sup>

## ABSTRACT

As a salt adsorbent, biochar could remove/isolate salt ions e.g. Na through physiochemical adsorption to mitigate the salinity of brackish water, but little is known about its magnitude and mechanisms. The current study aimed to examine the effects of biochar on: (1) Na-adsorptive capacity and mechanism and (2) Electrical Conductivity (EC) and K displacement. Six pyrolysis temperatures (250, 350, 450, 550, 650, and 750°C) were applied to produce biochars from rice husk. The biochars were then used as adsorbents to adsorb Na from salty water varying in NaCl concentrations. The Langmuir isotherm Model (LMM) and Dubinin-Radushkevick isotherm Model (DRM) were used to quantify the dependence of adsorbed Na on Na concentration at equilibrium. The LMM quantification revealed that the maximum Na-adsorptive capacity of biochars increased from 25.8 to 67.8 (mg g<sup>-1</sup>) upon increased temperatures. The EC was reduced and the K amount displaced from biochar was increased with an increase in pyrolysis temperature. The DRM quantification revealed that the Na-adsorptive mechanism was mainly a physical process. A significant relationship between the Na amount adsorbed and the K amount displaced from biochar suggested that the ion-exchange mechanism could co-exist. In brief, the findings indicated that the salinity of the brackish water could be significantly mitigated by the biochar treatment through mainly physical adsorption leading to a reduced EC and increased K: Na ratio.

**Keywords:** Dubinin-Radushkevick model, Langmuir isotherm, Saline soils, Sodium adsorption.

## INTRODUCTION

Climate change may increase seawater intrusion, which is one of a few reasons for degrading soils (Mingyi *et al.*, 2019) into salt-affected soils, occupying a large area over the world (Arora, 2017). Salt-affected

water is characterized by a high concentration of dissolved salts, especially sodium chloride, inducing negative impacts on plant growth. Although the brackish water may be important for agricultural production because of either intentional or unintentional use or seawater intrusion, insufficient studies have been conducted to

<sup>1</sup> Institute of Environmental Science, Engineering, and Management, Industrial University of Ho Chi Minh City, 12 Nguyen Van Bao, Go Vap District, Ho Chi Minh City, Vietnam.

<sup>2</sup> Institute for Chemistry and Materials, Academy of Military Science and Technology, 17- Hoang Sam, Nghia Do, Cau Giay, Hanoi, Vietnam.

<sup>3</sup> Faculty of Environment, Hanoi University of Mining and Geology, 18 Pho Vien, Duc Thang, Bac Tu Lien, Hanoi, Vietnam.

<sup>4</sup> HUTECH Institute of Applied Sciences, Ho Chi Minh City University of Technology (HUTECH), 475A, Dien Bien Phu, Ward 25, Binh Thanh District, Ho Chi Minh City, Vietnam.

<sup>5</sup> Faculty of History, University of Social Sciences and Humanities- Vietnam National University in Ho Chi Minh City, 10-12 Dinh Tien Hoang, Dist.1, Ho Chi Minh City, Vietnam.

\* Corresponding author; e-mail: [tv.nam@hutech.edu.vn](mailto:tv.nam@hutech.edu.vn)



treat/reduce the salinity of water for irrigation. Information of salinity reduction from salty water by organic amendment is scarce, but that from salt-affected soil is abundant (Hammer *et al.*, 2015, Gunarathne *et al.*, 2020).

Biochar, a carbon-rich substance possibly produced from agricultural residues, can be used as an organic amendment to reduce the salinity of the salt-affected soils (Saifullah *et al.*, 2018; Xiao and Meng, 2020). The authors also summarized various benefits brought to salt-affected soils through biochar addition, including reduced Na concentration and EC of the biochar-added soil. Lashari *et al.* (2013) reported that biochar addition significantly reduced Na concentration of the salt-affected soil from a two-year, on-field experiment. The reduced Na concentration and EC of the salt-affected soil could be explained with a few mechanisms, including Na adsorption on the amendment (Akhtar *et al.*, 2015). It can be assumed that biochar could have similar effects on brackish water, necessitating more studies.

It is also highlighted that the Na adsorption and EC reduction could be determined by the biochar's properties, which can be governed by feedstock and pyrolysis conditions such as temperature (Tomczyk *et al.*, 2020). The feedstock such as rice husk is much abundant in the rice-producing countries and thus is a potential source for biochar production. The pyrolysis temperature was reported to alter the physical and chemical properties of biochar (Rafiq *et al.* 2016, Li *et al.* 2017). These indicate that increasing pyrolysis temperature could produce biochars varying in properties, consequent Na adsorptive capacity, and EC-reducing effects. Nevertheless, our up-to-date literature search revealed that studies addressing the Na-adsorptive capacity of biochar produced at different pyrolysis temperatures are insufficient.

In general, the Na adsorption could be controlled by physical and chemical mechanisms, which can be identified

through an adsorption isotherm model, called Dubinin-Radushkevick (Olalekan *et al.*, 2010, Taha *et al.*, 2017). For an adsorptive event, both mechanisms could likely occur concurrently and vary in proportion with biochars produced at different pyrolysis temperatures. Na adsorption may lead to a change in the EC and displacement of K from the biochar to the solution. Nevertheless, such information from literature was discussed insufficiently, necessitating more study to clarify.

Therefore, the current study was conducted to examine the effects of biochar produced at different temperatures on: (1) Na-adsorptive capacity and mechanism, and (2) Electrical Conductivity (EC) and K displacement. It was hypothesized that an increase in pyrolysis temperature would result in a higher Na-adsorptive capacity of biochar, increase potassium displacement, and reduce the electrical conductivity of the salty solution.

## MATERIALS AND METHODS

Rice husk, collected from rice-milling plants, was washed with tap water, air-dried for a few days, and oven-dried at 70°C overnight before pyrolysis. The oven-dried husk was placed in a ceramic cup covered with a lid and subjected to pyrolysis using an electrical muffle furnace. The furnace was programmed to increase from room temperature at a heating rate of 10°C per minute to the targeted temperatures and held there for 4 hours. Six targeted temperatures, including 250, 350, 450, 550, 650, and 750°C were applied to produce biochar, based on some studies (Lehmann and Joseph, 2009; Zhang *et al.*, 2017; Elnour *et al.*, 2019; Guilhen *et al.*, 2019). After pyrolysis, the furnace was turned off and the cup was left inside for about 2 hours to cool to room temperature. The formed biochars were labeled as 250-BC, 350-BC, 450-BC, 550-BC, 650-BC, and 750-BC and stored in a plastic bag for the adsorption experiment.

**Table 1.** Selected properties of biochars produced at 250, 350, 450, 550, 650, and 750 °C.

Biochars (BC)	Statistics <sup>a</sup>	Ash content (%)	pH	EC ( $\mu\text{S cm}^{-1}$ )	Na	K	Ca
					(cmole(+) kg <sup>-1</sup> )		
250-BC	Mean	12.92	7.20	399.04	1.23	1.56	3.70
	SE	0.13	0.06	5.74	0.01	0.02	0.03
350-BC	Mean	22.40	7.30	320.00	1.95	2.68	5.49
	SE	0.35	0.00	3.21	0.01	0.05	0.02
450-BC	Mean	25.80	7.67	417.29	3.46	4.38	8.83
	SE	1.58	0.07	2.30	0.03	0.03	0.07
550-BC	Mean	34.81	8.00	453.00	2.82	4.17	8.02
	SE	0.59	0.06	1.15	0.01	0.06	0.01
650-BC	Mean	34.75	8.23	429.05	3.34	4.15	9.11
	SE	0.53	0.07	1.78	0.04	0.04	0.07
750-BC	Mean	33.96	8.47	426.31	2.96	4.17	8.20
	SE	0.24	0.03	6.92	0.02	0.04	0.04

<sup>a</sup> SE= Standard deviation of the mean (n= 3).

Some selected properties of these biochars were shown in Table 1.

### Biochar Adsorption Experiment

The adsorption experiment was carried out by weighing 1.5 gram of each biochar into a 50-mL centrifuge tube containing 30-mL NaCl solution, varying in NaCl concentrations of 0, 0.25, 0.5, 1.0, 2.0, and 3.5%, equal to 0, 1,438, 2,875, 5,750, 11,500, and 20,125 mg Na<sup>+</sup> L<sup>-1</sup>, respectively. These NaCl concentrations may form solutions with EC values varying from 0, 4.0, 8.0, 16, 31.5, and 55 dS m<sup>-1</sup>, respectively. These EC values corresponded to the thresholds set by Richards (1954) to classify soil salinity (< 2, 2-4, 4-8, 8-16 dS m<sup>-1</sup>), while the concentration of 3.5% with a 55 dS m<sup>-1</sup> EC was similar to that of the seawater (Schnepf *et al.*, 2014). Although the two highest salt concentrations in the current study can be high compared to brackish water, they are still selected because the seawater intrusion may bring the seawater to agricultural fields and they are necessary for estimating the maximum adsorption capacity of the tested biochars. The sample tubes were then placed on a horizontal shaker for 24 hours and allowed to settle for 1 hour at room temperature. The

supernatants from the sample tubes were filtered with Whatman filter paper into centrifuge tubes and immediately measured for EC. The filtrate in the tubes was then acidified by adding 3 drops of HNO<sub>3</sub>, and stored in a 4°C refrigerator until measuring Na and K concentration. The adsorption experiment was conducted in three replicates, with a total of 108 samples [6 (biochars)×6 (solutions with 6 initial Na concentrations) × 3 (replicates)] for the experiment.

### Chemical Analysis

Six biochars were ground to pass 2 mm-sieve before measuring for pH, EC, Na, K, Ca, and ash content. For pH and EC, the materials received distilled water at 1:5 (w/w) ratio and the extracts were measured for pH and EC using pH meter and EC meter, respectively. The total concentrations of Na, K, and Ca were measured using the digestion method ( Nguyen and Lehmann, 2009) and the extracted solution was analyzed using an Inductively Coupled Plasma spectroscopy–Optical Emission Spectrometer (ICP-OES, Spectro Analytical Instrument GmbH, 47533 Kleve Germany). Ash content was measured by heating 2 grams of individual biochar at 600°C



overnight. All these measurements were carried out in three replicates. EC of the 108 filtered solutions after the adsorption experiment and of 18 initial salty solutions (6 NaCl concentrations  $\times$  3 replicates) was measured using an EC meter. Na and K concentrations of the 108 acidified filtered solutions were measured using ICP-OES.

### Modeling and Statistical Analyses

The amount of Na adsorbed by biochars depended on the Na concentration at equilibrium and was quantified using the Langmuir isotherm Model (LMM) and Dubinin-Radushkevich isotherm Model (DRM). The LMM can be written as Equation (1):

$$q_e = \frac{Q_m K_L C_e}{1 + K_L C_e} \quad (1)$$

Where,  $q_e$  is the amount of Na adsorbed on biochar at equilibrium ( $\text{mg g}^{-1}$ );  $Q_m$  is the maximum capacity of biochar ( $\text{mg g}^{-1}$ );  $K_L$  is the Langmuir isotherm constant or adsorption energy ( $\text{L g}^{-1}$ ), and  $C_e$  is the equilibrium concentration of Na ( $\text{mg L}^{-1}$ ).  $q_e$  was calculated through the Equation (2):

$$q_e = \frac{v(c_i - c_e)}{w} \quad (\text{Vanderborgh and Grieken 1977}) \quad (2)$$

Where,  $v$  is the used volume of Na solution;  $c_i$  and  $c_e$  are Na concentration before adsorption and at equilibrium, respectively ( $\text{mg g}^{-1}$ );  $w$  is the weight (gram) of biochar used. Data from the current study was also used to examine the adsorption mechanisms, using the Dubinin-Radushkevich isotherm Model (DRM) (Equation 3).

$$q_e = q_s e^{-K_{ad} \varepsilon^2} \quad (3)$$

Where,  $q_e$  is the amount of Na adsorbed on biochar at equilibrium ( $\text{mg g}^{-1}$ );  $q_s$  is the theoretical isotherm maximum capacity ( $\text{mg g}^{-1}$ );  $K_{ad}$  is the Dubinin-Radushkevich isotherm constant ( $\text{mol}^2 \text{kJ}^2$ ) related to the adsorption energy, and  $\varepsilon$  is Polanyi potential ( $\text{kJ mol}^{-1}$ ) and can be computed as Equation (4):

$$\varepsilon = RT \ln \left( 1 + \frac{1}{C_e} \right) \quad (4)$$

Where,  $R$ ,  $T$ , and  $C_e$  are the universal gas constant ( $8.314, \text{J mol}^{-1} \text{K}^{-1}$ ), absolute Temperature (K), and Na equilibrium Concentration ( $\text{mg L}^{-1}$ ), respectively. From  $K_{ad}$ , the Gibbs free energy of biochar ( $E$ ) can be computed as  $E = \frac{1}{\sqrt{2K_{ad}}}$  ( $\text{kJ mol}^{-1}$ ) (Mane *et al.*, 2007). If the  $E$  value was lower than  $8 \text{ (kJ mol}^{-1}\text{)}$  the adsorption was a physical process, and if  $E$  was between  $8$  and  $16 \text{ (kJ mol}^{-1}\text{)}$ , it was a chemical process (Taha *et al.*, 2017). In addition, simple linear regression and exponential functions were also carried out to examine various relationships among measured parameters. All figures and model fittings were carried out using Sigmaplot 12 (Systat Software Inc.). More details about modeling and statistical analyses are shown in the Supplementary Material.

## RESULTS

### Sodium Adsorption on Biochars

Figure 1 shows that with an increase in initial Na concentration in the tested solution, the amount of Na adsorbed on biochars increased exponentially, rapidly for the initial Na concentrations lower than  $11,500 \text{ (mg L}^{-1}\text{)}$  of  $\text{Na}^+$  (equal to 2% NaCl) but leveled off for the concentrations higher than  $11,500 \text{ (mg L}^{-1}\text{)}$  of  $\text{Na}^+$ . Of the 6 biochars produced, at the lowest temperature  $250^\circ\text{C}$  adsorbed Na the least, and that produced at  $750^\circ\text{C}$  adsorbed the greatest.

The maximum adsorption capacity of the 250-BC was the lowest ( $25.8 \text{ mg g}^{-1}$ ) and that of the 750-BC was the highest ( $67.8, \text{ mg g}^{-1}$ ), estimated by the LMM (Table 2). All  $E$  values of the tested biochars estimated through the DRM were lower than  $8 \text{ (kJ mol}^{-1}\text{)}$ , indicating that the adsorptive mechanism was a physical process. Table 2 also shows that the LMM and the DRM were suitable to use for modeling the Na adsorption isotherm of biochar due to higher values of  $R^2$  ( $> 0.93$ ). The maximum adsorption capacity of biochars, estimated

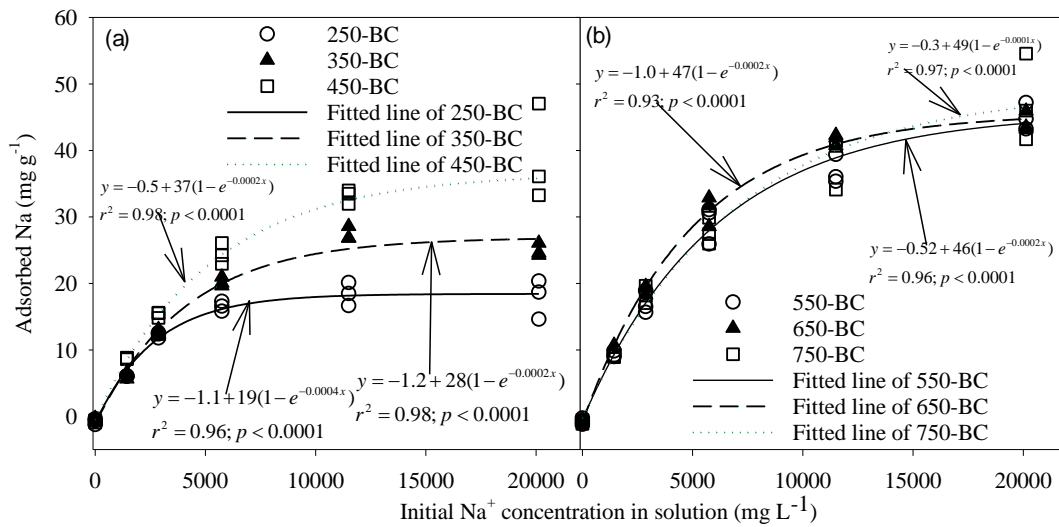


**Figure 1.** Relationship between the amount of Na adsorbed on six biochars and initial concentration of Na in solution.

**Table 2.** Parameters of Langmuir and Dubinin–Radushkevich Isotherm models for Na adsorption on six biochars.

Biochars (BC)	Langmuir isotherm (LMM)				Dubinin–Radushkevich isotherm (DRM)			
	Qm (mg g <sup>-1</sup> )	L <sub>L</sub> (L g <sup>-1</sup> )	R <sub>L</sub>	R <sup>2</sup>	q <sub>s</sub> (mg g <sup>-1</sup> )	K <sub>ad</sub> (mol <sup>2</sup> kJ <sup>-2</sup> )	E (kJ mol <sup>-1</sup> )	R <sup>2</sup>
250-BC	25.8	0.00030	0.50	0.935	17.6	0.23	1.49	0.960
350-BC	45.6	0.00015	0.61	0.975	23.2	0.29	1.33	0.981
450-BC	48.8	0.00022	0.54	0.998	29.5	0.21	1.55	0.958
550-BC	60.5	0.00020	0.57	0.992	34.0	0.21	1.57	0.957
650-BC	61.2	0.00023	0.54	0.995	36.3	0.18	1.67	0.975
750-BC	67.8	0.00016	0.60	0.982	35.4	0.22	1.49	0.968

by two isotherm models was significantly increased with an increase in pyrolysis temperature (Figure 2-a). The averaged capacity increased from 25 to 66 (mg g<sup>-1</sup>) estimated with the LMM and from 17 to 36 (mg g<sup>-1</sup>) estimated with the DRM. The LMM constant or adsorption energy of the 6 tested biochars was low, varied insignificantly, and was lower than that of DRM free energy (Figure 2-b).

### Electrical Conductivity and Potassium Displacement

With an increase in initial Na concentration from 0 to 20125 (mg L<sup>-1</sup>), the EC value of the no-biochar added solution increased significantly from 0 to 54 (dS m<sup>-1</sup>)

(Figure 3-a). The increasing trend was modeled into a linear regression equation with a slope coefficient of 0.0027 (dS m<sup>-1</sup> mg L<sup>-1</sup>) and r<sup>2</sup>= 0.98. The addition of biochars produced at different temperatures reduced EC values of the tested solutions relative to the no-BC added solution (Figures 3-a, -b, and -c). The increasing patterns of EC from the biochar-added solutions followed an exponential-rise-to-maximum model i.e.

$$(y = a + b(1 - e^{-bx})) \quad (5)$$

Where, b is the maximum value of EC that the solution could reach.

The b value decreased from 74 dS m<sup>-1</sup> in 250-BC to 25 dS m<sup>-1</sup> in 750-BC.

With an increase in initial Na concentration in the salty solution, the quantity of K displaced from biochars was increased exponentially,

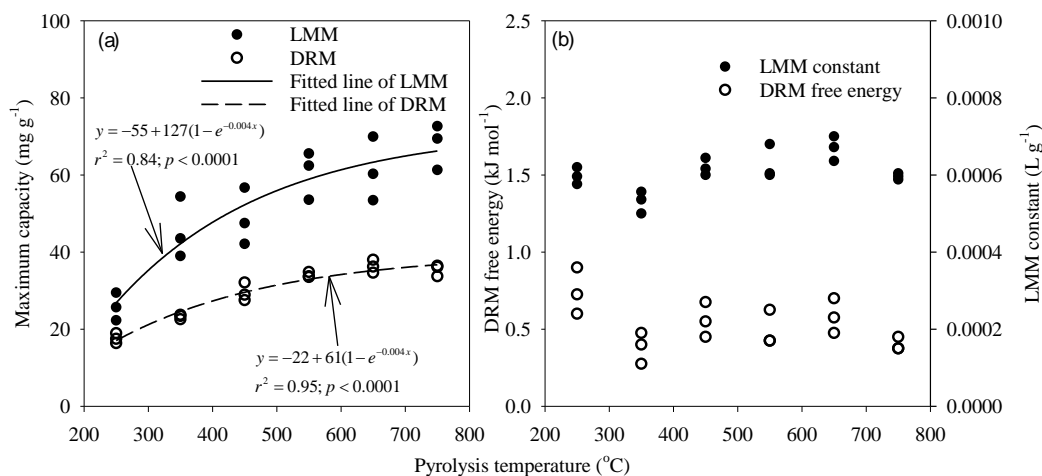


**Figure 2.** The relationship between (a) Maximum adsorption capacity and (b) DRM free energy and LMM constant of biochars with pyrolysis temperatures. Only a significant relationship (a) was shown with a fitted equation. (LMM = Langmuir isotherm Model, DRM= Dubinin-Radushkevich isotherm Model).

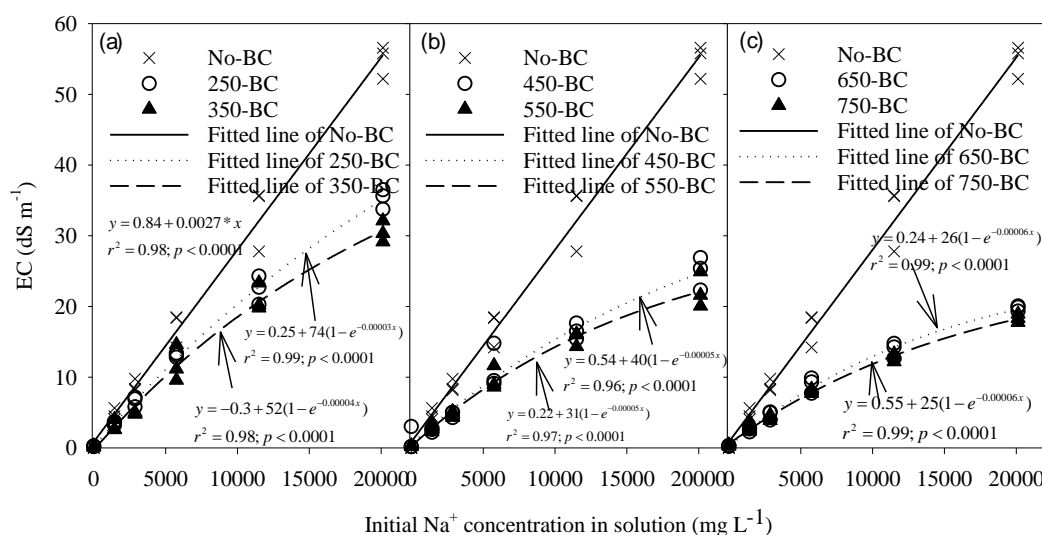


**Figure 3.** The relationship between the electrical conductivity of Biochars (BC) with the initial concentration of Na in solution.

depending on pyrolysis temperature (Figures 4-a and -b). For the temperatures from 250 to 650°C, the release rate of K from biochar increased rapidly, while for the temperatures from 650 to 750°C, that rate leveled off. With increase in pyrolysis temperature from 250 to 750°C, the maximum release rate of K from biochar increased from 0.93 to 4.3 (mg g<sup>-1</sup>).

The adsorbed quantity of Na on biochars was significantly correlated with the displaced quantity of K from biochars

(Figures 5-a and -b) and with the reduced magnitude of EC in the tested solution (Figures 5-c and -d). The relationship between adsorbed Na and displaced K was a three-parameter exponential-rise-to-maximum model; the rapidly increasing phase was observed for the lower levels of the K quantity displaced from biochars. The relationship between the adsorbed Na with the reduction of solution EC was modeled into a three-parameter exponential-growth

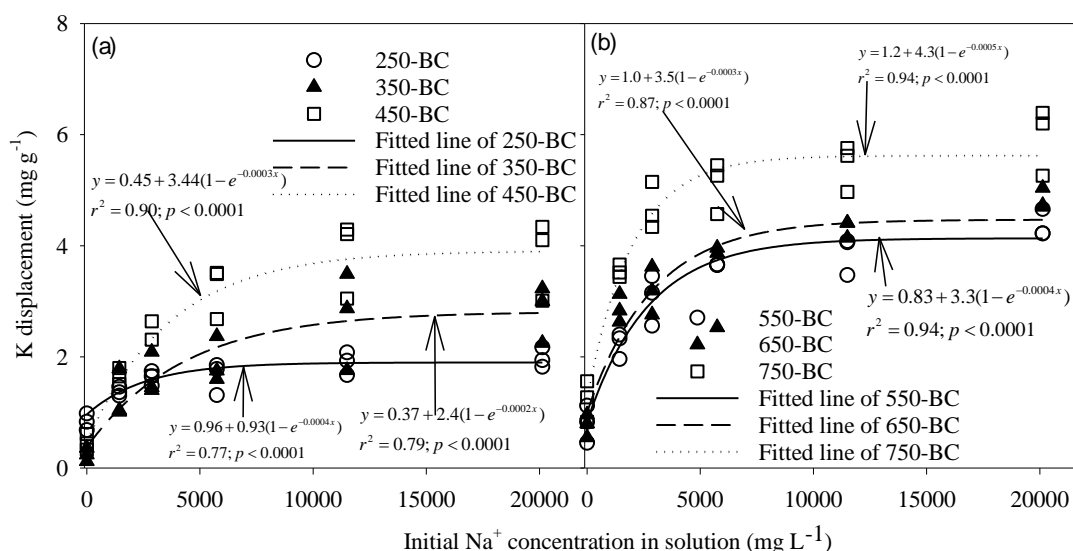


**Figure 4.** The relationship between potassium displaced from 6 biochars with the initial concentration of Na in solution.

pattern. For the adsorbed quantity of Na lower than 10 mg g<sup>-1</sup>, the EC reduction rate increased slowly, but for higher quantities of adsorbed Na, the EC reduction rate increased rapidly. Increasing pyrolysis temperature led to a reduction in EC at all levels of adsorbed Na, except for the lowest one, at which EC was increased with the addition of biochar.

## DISCUSSION

### Sodium Adsorption Capacity and Mechanisms of Biochars

The current study found that the maximum adsorption capacity of biochars for Na varied from 26 in 250-BC to 68 (mg g<sup>-1</sup>) in 750-BC and the varying pattern was an exponential-rise-to-maximum model. Although limited studies have been conducted to address the Na adsorption capacity of biochar, these numbers were similar to the other findings by other authors. Akhtar *et al.* (2015) found that biochar produced from a mixture of hardwood and softwood at 500°C was able

to adsorb as much as 60-mg Na<sup>+</sup> per gram biochar. Using feedstock of rice husk similar to the current study, Rostamian *et al.* (2015) found that biochars produced at 400, 600, and 800°C had a maximum Na adsorption capacity of 35, 61, and 54 mg g<sup>-1</sup>, which were within the capacity range found in the current study based on the LMM. The increased Na adsorptive capacity of biochars in the current study could be explained by the physical and chemical properties of biochars determined by pyrolysis temperature. Physically, Tushar *et al.* (2012) concluded that the increased pyrolysis temperature improved the porosity and subsequently high surface area of biochar. Similarly, an increase in pyrolysis temperature was reported to produce biochars with a higher BET (Brunauer–Emmett–Teller) surface area (Rafiq *et al.*, 2016). Because the adsorption is proportional to the surface of the open portion of the adsorbent (Giron *et al.* 2002), the increased surface area of biochars would enhance Na adsorptive capacity estimated by the LMM. Likewise, Rostamian *et al.* (2015) found that the surface area of biochar was significantly correlated with Na adsorptive

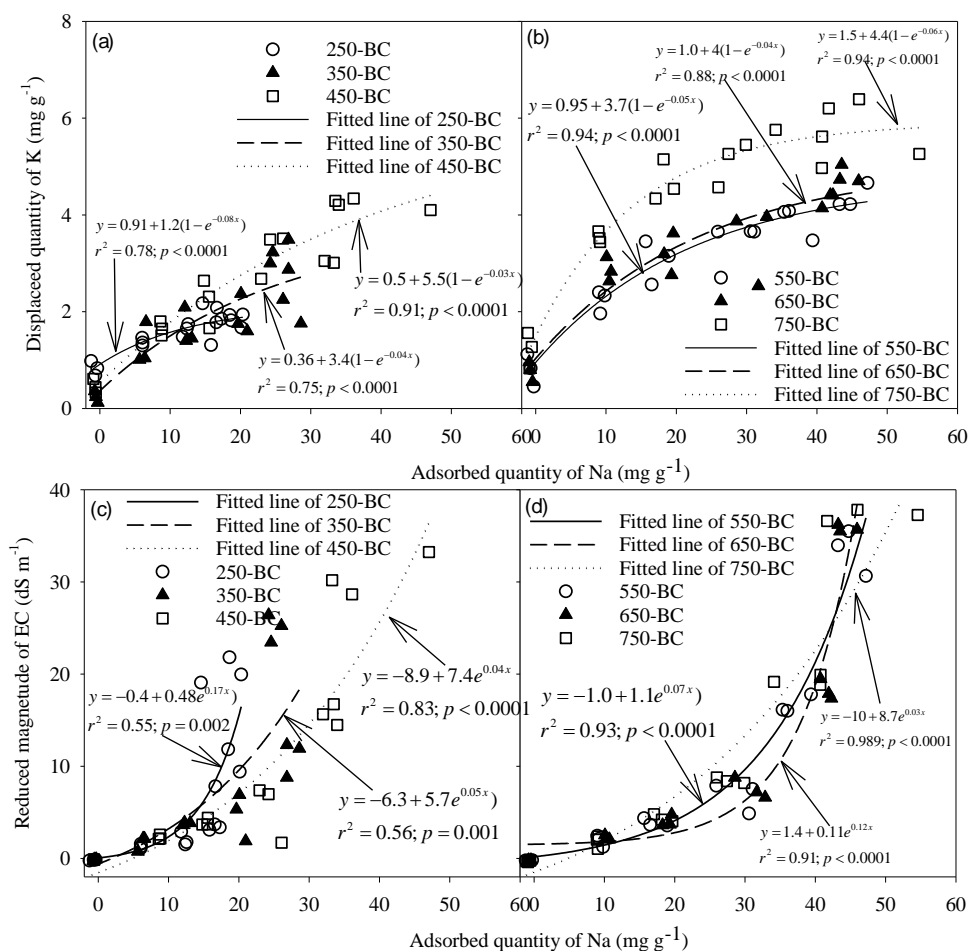


**Figure 5.** The relationship between the amount of K displaced with the amount of Na adsorbed on 6 biochars (a, b) and between the reduced magnitude of EC and the amount of Na adsorbed on 6 biochars (c, d).

capacity due to the movement of ions from the environmental solution to the surface of biochar particles.

Chemically, Na could be adsorbed on biochar's surface through exchangeable sites, which are negatively charged, or through polar organic functional groups (Banik *et al.*, 2018). A decrease in total functional groups such as carboxylic, amino, and hydroxyl groups of biochar as a result of increased pyrolysis temperature (Li *et al.*, 2017) may suggest that Na adsorptive capacity would be a decreasing pattern upon increasing pyrolysis temperature. The increase in Na adsorption capacity with pyrolysis temperature from the current study indicated that Na adsorption could be

determined by physical rather than chemical processes.

The physical mechanism was predominant in determining the Na adsorption of biochar because the Gibbs free Energy of biochar (E) varied from 1.33 to 1.67 (kJ mol<sup>-1</sup>) (Table 2), lower than 8 (kJ mol<sup>-1</sup>) (Taha *et al.*, 2017). The physical adsorption mechanism is greatly dependent on the biochar's specific surface area, on which Na can be adsorbed and diffused into the micropores of biochars (Yang *et al.* 2019). As a result, an increase in specific surface area of biochars upon increasing pyrolysis temperature (Rafiq *et al.*, 2016) could account for the increase in Na adsorptive capacity following physical adsorptive



mechanism as shown in Table 2 and Figure 2-a. Additionally, other adsorptive mechanisms such as electrostatic ion exchange could be present in the current study. The mechanism, i.e. the exchange of ions such as  $H^+$  or base cations such as  $Na^+$ ,  $K^+$ , and  $Ca^{2+}$  of biochar with those from solution (Yang *et al.*, 2019), could be inferred from the significant correlation between the adsorbed quantity of Na and the displaced amount of K (Figures 5-a and -b). This mechanism could represent as much as 10 to 39% (computed as  $(\frac{\text{displaced amount of K}}{\text{adsorbed amount of Na}} \times 100)$ ) of total Na adsorbed on biochars, depending on pyrolysis temperatures.

The current study also found that, at every pyrolysis temperature, the maximum Na adsorptive capacity of biochar estimated by the LMM was much higher than that estimated by the DRM. The difference was also found by other studies (Dada *et al.* 2012). Chen (2015) reported that the maximum capacity estimated by the LMM of four tested adsorbents was higher than that estimated by the DRM. Although the real reasons accounting for the difference in maximum absorption capacity by the two models are still unclear, it could be related to the models' assumptions, in which the adsorption through the Langmuir isotherm can take place at specific homogeneous sites with an adsorptive monolayer, while that through the Dubinin-Radushkevich isotherm can occur onto both homogeneous and heterogeneous surfaces (Chen, 2015; Nebaghe *et al.*, 2016). In addition, the Dubinin-Radushkevich isotherm was established to focus more on the pore-filling mechanism of the adsorptive process, while the Langmuir isotherm was formulated to originally describe the gas-solid phase adsorption but also was used to quantify the maximum adsorptive capacity of various adsorbents (Ayawei *et al.*, 2017).

### Change in Electrical Conductivity

Biochars produced at higher pyrolysis temperatures reduced EC values of the tested solution more than those produced at lower temperatures (Figure 3). The reduced

magnitude of EC was significantly related to Na adsorption of the biochar; more Na adsorbed resulted in lower EC. Similarly, conducting a pot experiment on soil added with NaCl to have EC of  $1.3 \text{ dS m}^{-1}$ . Hammer *et al.* (2015) found that biochar addition reduced the soil's EC. The biochar EC varied greatly, depending on feedstock and pyrolysis temperature, ranging from 0.04 (Rajkovich *et al.*, 2011) to as high as  $54.2 \text{ dS m}^{-1}$  (Smider and Singh, 2014). Consequently, Saifullah *et al.* (2018) hypothesized that the EC of salt-affected soil could be increased or decreased, basically depending on the relative EC of the soil solution and of the biochar. Relative to the solution, high-EC biochar may increase the solution EC, while low-EC biochar may reduce the solution EC. This could be in line with the current study. For the solution added without salt (the zero-NaCl treatment), biochar addition increased the EC of the solution, while for the other solutions added with salt, biochar addition reduced the EC of the tested solution (Figures 3-a, -b, -d and 5-c, -d). The increased EC of the no-salt-added solution could be due to the release of salts from biochar, typically K, Ca, and other cations.

### 4.3. Potassium Displacement and Others

The current study found that the quantity of K displaced from biochar was higher in the biochar produced at higher pyrolysis temperature (Figures 4-a and -b), indicating that high pyrolysis temperature led to a higher K content of the resultant biochar. Naeem (2014) and Titiladunayo *et al.* (2012) reported similar results and the reason could be the low vaporization temperature of organic C, leading to more organic C loss, relative to that of K. With an increase in the initial Na concentration in the tested solution, more K was displaced into the solution (Figures 4-a and -b). Because of similar physicochemical properties, K and Na could compete for adsorptive sites on the biochars, resulting in a significant relationship between the Na amount adsorbed on and the K amount displaced from the tested biochars. Nevertheless, the



stoichiometric ratio of the displaced K to adsorbed Na in the current study varied from 0.1:1 to 0.39:1, instead of 1:1. This may indicate that part of the K on the biochar was a bit strongly bound to the biochar structure that needed a stronger repulsive force from the Na competency (higher Na concentration in the tested solution) to push it into the solution.

Although the current study did not measure the Ca concentration of the salty solution after the adsorption experiment, the Ca content of biochar may affect the Na adsorption and EC of the salty solution. The Ca concentration of biochar was increased with pyrolysis temperature, and was higher than the Na and K concentration (Table 1). Some materials may retain Na in a high preference over Ca (Singh *et al.*, 2018), indicating that Ca could be more displaced from the adsorbent into the salty solution. This may also suggest that biochar addition to sodic soils or saline and sodic soils may improve the soil quality by lowering the sodium adsorption ratio.

The current study found some interesting results for using biochar produced at different pyrolysis temperatures as an adsorbent to mitigate some characteristics of brackish water and possibly salt-affected soils. Nevertheless, this is an adsorption experiment, conducted in a laboratory for 24 hours, which may not reflect the real effects of biochar in fields. Greenhouse and open-field experiments are needed to verify the effects. Additionally, structural analysis of the tested biochar should be implemented to explain the findings related to the adsorption characteristics.

## CONCLUSIONS

The current study revealed that the Na adsorption capacity of biochar was significantly correlated with pyrolysis temperature, increasing from 25.8 at 250°C to 67.8 (mg g<sup>-1</sup>) at 750°C following an exponential-rise model. The EC of the tested solution was reduced by biochars produced

at different temperatures and was significantly correlated with the amount of Na adsorbed on biochar. Following the Na adsorption, K displacement from biochar was significantly correlated with pyrolysis temperature and with the Na quantity adsorbed on biochars. The result from the Dubinin-Radushkevich isotherm model revealed that the Na adsorptive mechanism was mainly a physical process. The significant correlation between the Na amount adsorbed and the K amount displaced from biochar may additionally suggest that the ion-exchange mechanism could co-exist and may be responsible for 10-39% of the adsorbed Na. Biochar produced at 450 to 550°C showed as a promising organic amendment in Na adsorption and EC reduction of the brackish water. In brief, as a result of increasing pyrolysis temperature, the maximum Na adsorptive capacity of biochars was increased, accompanied by an increase in the quantity of K displaced from biochar, while EC of the solution was reduced accordingly.

## ACKNOWLEDGEMENTS

This work was financially supported by the Department of Science and Technology of Ho Chi Minh City under contract No. 36/2020/HĐ-QPTKHCN, signed on July 13, 2020. The authors are grateful to the Industrial University of Ho Chi Minh City (IUH) and the Institute of Environmental Science, Engineering, and Management (IESEM) of IUH. Many thanks are given to the staff and students at IESEM for their help with field trips.

## REFERENCES

1. Akhtar, S.S., Andersen, M.N. and Liu, F. 2015. Biochar Mitigates Salinity Stress in Potato. *J. Agron. Crop Sci.*, **201(5)**: 368-378.
2. Arora, S. 2017. Diagnostic Properties and Constraints of Salt-Affected Soils. In "Bioremediation of Salt Affected Soils: An

- Indian Perspective*" (Eds): Arora, S., Singh, A. K. and Singh, Y. P. Springer International Publishing, Cham, PP. 41-52.
3. Ayawei, N., Ebelegi, A.N. and Wankasi, D. 2017. Modelling and Interpretation of Adsorption Isotherms. *J. Chem.*, Article ID **3039817**: 11 PP.
  4. Banik, C., Lawrinenko, M., Bakshi, S. A. and Laird, D. 2018. Impact of Pyrolysis Temperature and Feedstock on Surface Charge and Functional Group Chemistry of Biochars. *J. Environ. Qual.*, **47(3)**: 452-461
  5. Chen, X. 2015. Modeling of Experimental Adsorption Isotherm Data. *Information*, **6**: 14-22.
  6. Dada, A. O., Olalekan, A., Olatunya, A. and Dada, A. O. 2012. Langmuir, Freundlich, Temkin and Dubinin–Radushkevich Isotherms Studies of Equilibrium Sorption of Zn<sup>2+</sup> onto Phosphoric Acid Modified Rice Husk. *J. Appl. Chem.*, **3**: 38-45.
  7. Elnour, A., Alghyamah, A., Shaikh, H., Poulouse, A., Al-zahrani, S., Anis, A. and Al-Wabel, M. 2019. Effect of Pyrolysis Temperature on Biochar Microstructural Evolution, Physicochemical Characteristics, and Its Influence on Biochar/Polypropylene Composites. *Appl. Sci.*, **9**: 1149.
  8. Giron, D., Goldbronn, C., Mutz, M., Pfeffer, S., Piechon, P. and Schwab, P. 2002. Solid State Characterizations of Pharmaceutical Hydrates. *J. Therm. Anal. Calorim.*, **68(2)**: 453-465.
  9. Guilhen, S., Masek, O., Ortiz, N., Izidoro, J. and Fungaro, D. 2019. Pyrolytic Temperature Evaluation of Macauba Biochar for Uranium Adsorption from Aqueous Solutions. *Biomass Bioenerg.*, **122**: 381-390.
  10. Gunarathne, V., Senadeera, A., Gunarathne, U., Biswas, J.K., Almaroai, Y.A. and Vithanage, M. 2020. Potential of Biochar and Organic Amendments for Reclamation of Coastal Acidic-Salt Affected Soil. *Biochar*, **2(1)**:
  11. Hammer, E. C., Forstreuter, M., Rillig, M. C. and Kohler, J. 2015. Biochar Increases Arbuscular Mycorrhizal Plant Growth Enhancement and Ameliorates Salinity Stress. *Appl. Soil Ecol.*, **96(Suppl. C)**: 114-121.
  12. Lashari, M. S., Liu, Y., Li L., Pan, W., Fu, J., Pan, G., Zheng, J., Zheng, J., Zhang, X. and Yu, X. 2013. Effects of Amendment of Biochar-Manure Compost in Conjunction with Pyrolygneous Solution on Soil Quality and Wheat Yield of a Salt-Stressed Cropland from Central China Great Plain. *Field Crop. Res.*, **144**: 113-118.
  13. Lehmann, J. and Joseph, S. 2009. Biochar for Environmental Management: An Introduction. In: "*Biochar for Environmental Management*", (Eds.): Lehmann, J. and Joseph, S. Earthscan in the UK, Dunstan House, London, EC1N 8XA, UK, PP. 1-12.
  14. Li, H., Dong, X., da Silva, E. B., de Oliveira, L. M., Chen, Y. and Ma, L. Q. 2017. Mechanisms of Metal Sorption by Biochars: Biochar Characteristics and Modifications. *Chemosphere*, **178**: 466-478.
  15. Mane, V. S., Deo Mall, I. and Chandra Srivastava, V. 2007. Kinetic and Equilibrium Isotherm Studies for the Adsorptive Removal of Brilliant Green Dye from Aqueous Solution by Rice Husk Ash. *J. Environ. Manage.*, **84(4)**: 390-400.
  16. Mingyi, H., Zhang, Z., Zhai, Y., Peirong, L. and Zhu, C. 2019. Effect of Straw Biochar on Soil Properties and Wheat Production under Saline Water Irrigation. *Agronomy*, **9**: 457.
  17. Naeem, M. A. 2014. Yield and Nutrient Composition of Biochar Produced from Different Feedstocks at Varying Pyrolytic Temperatures. *Pak. J. Agric. Sci.*, **51**: 75-82.
  18. Nebaghe, K. C., El Boundati, Y., Ziat, K., Naji, A., Rghioui, L. and Saidi, M. 2016. Comparison of Linear and Non-Linear Method for Determination of Optimum Equilibrium Isotherm for Adsorption of Copper(II) onto Treated Martil Sand. *Fluid Phase Equilibria*, **430**: 188-194.
  19. Nguyen, B. T. and Lehmann, J. 2009. Black Carbon Decomposition under Varying Water Regimes. *Organic Geochem.*, **40(8)**: 846-853.
  20. Olalekan, A. P., Dada, A. O. and Okewale, A. O. 2010. Sorption Energies Estimation Using Dubinin-Radushkevich and Temkin Adsorption Isotherms. *Life Sci. J.*, **7**: 68.
  21. Rafiq, M., Bachmann, R., Rafiq, M. T., Shang, Z., Joseph, S. and Long, R. 2016. Influence of Pyrolysis Temperature on Physico-Chemical Properties of Corn Stover (*Zea mays* L.) Biochar and Feasibility for Carbon Capture and Energy Balance. *PLoS ONE*, **11**: e0156894.
  22. Rajkovich, S., Enders, A., Hanley, K., Hyland, C., Zimmerman, A. and Lehmann, J. 2011. Corn Growth and Nitrogen



- Nutrition after Additions of Biochars with Varying Properties to a Temperate Soil. *Biol. Fertil. Soil.*, **48**: 271–284.
23. Richards, L. A. 1954. *Diagnosis and Improvement of Saline Alkali Soils*. USDA Handbook No. 60. Washington, DC, USA.
24. Rostamian, R., Heidarpour, M., Mousavi S. F. and Majid, A. 2015. Characterization and Sodium Sorption Capacity of Biochar and Activated Carbon Prepared from Rice Husk. *J. Agr. Sci. Tech.*, **17**: 1057-1069.
25. Saifullah, Dahlawi, S., Naeem, A., Rengel, Z. and Naidu, R. 2018. Biochar Application for the Remediation of Salt-Affected Soils: Challenges and Opportunities. *Sci. Total Environ.*, **625**: 320-335.
26. Schnepf, N.R., Manoj, C., Kuvshinov, A., Toh, H. and Maus, S. 2014. Tidal Signals in Ocean-Bottom Magnetic Measurements of the Northwestern Pacific: Observation versus Prediction. *Geophys. J. Int.*, **198**(2): 1096-1110.
27. Singh, B., Srivastava, P. and Shrivastava, M. 2018. Calcium-Sodium Exchange Equilibria in Two Soils of Chambal Command Area of Rajasthan, India. *Land Degrad. Dev.*, **29**(8): 2739-2745.
28. Smider, B. and Singh, B. 2014. Agronomic Performance of a High ash Biochar in Two Contrasting Soils. *Agric. Ecosys. Environ.*, **191**: 99-107
29. Taha, A. A., Ahmed, A. M., Abdel Rahman, H. H., Abouzeid, F. M. and Abdel Maksoud, M. O. 2017. Removal of Nickel Ions by Adsorption on Nano-Bentonite: Equilibrium, Kinetics, and Thermodynamics. *J. Dispers. Sci. Technol.*, **38**(5): 757.
30. Titiladunayo, I. F., McDonald, A. G. and Fapetu, O. P. J. W. 2012. Effect of Temperature on Biochar Product Yield from Selected Lignocellulosic Biomass in a Pyrolysis Process. *Waste Biomass Valori.*, **3**(3): 311-318.
31. Tomczyk A., Sokołowska Z. and Boguta P. 2020. Biochar Physicochemical Properties: Pyrolysis Temperature and Feedstock Kind Effects. *Rev. Environ. Sci. Bio/Technol.*, **19**(1): 191-215.
32. Tushar, H. K. M. S., Mahinpey, N., Khan, A., Ibrahim, H., Kumar, P. and Idem, R. 2012. Production, Characterization and Reactivity Studies of Chars Produced by the Isothermal Pyrolysis of Flax Straw. *Biomass Bioenerg.*, **37**: 97-105.
33. Vanderborght, B. M. and Grieken R. E. 1977. Enrichment of Trace Metals in Water by Adsorption on Activated Carbon. *Anal. Chem.*, **49**(2): 311-6.
34. Xiao, L. and Meng, F. 2020. Evaluating the Effect of Biochar on Salt Leaching and Nutrient Retention of Yellow River Delta Soil. *Soil Use Manage.*, **36**(4): 740-750.
35. Yang, X., Zhang, S., Ju, M. and Liu, L. 2019. Preparation and Modification of Biochar Materials and Their Application in Soil Remediation. *Appl. Sci.*, **9**: 1365.
36. Zhang, H., Chen, C., Gray, E. M. and Boyd, S. E. 2017. Effect of Feedstock and Pyrolysis Temperature on Properties of Biochar Governing End Use Efficacy. *Biomass Bioenerg.*, **105**: 136-146.

## پتانسیل بیوچار به دست آمده از پسماندهای کشاورزی به عنوان جاذب نمک برای بهسازی آبهای لب شور برای آبیاری

ب. تانها نگوین، گ. دای دینه، ت. زوان نگوین، د. دوان دو، د. توی فوک نگوین، ا. هونگ لی، ت. تگوک وو، ه. تو تی تران، ن. ون تایی، و ک. ون لوو

### چکیده

بیوچار به عنوان یک جاذب نمک می تواند یونهای نمک، مثلاً سدیم، را با فرایند فیزیکوشیمیایی جذب سطحی از محیط خارج یا جدا کرده و باعث بهسازی آبهای لب شور شود، ولی مطلب کمی در باره سازوکار و موثر بودن آن در دسترس است. هدف این پژوهش بررسی اثرات بیوچار بود بر (1) ظرفیت جذب سطحی سدیم و سازوکار آن و بر (2) هدایت الکتریکی (EC) و جابجا شدن پتاسیم (K). برای تهیه بیوچار از پوسته برنج، شش درجه حرارت برای آتشکافت (pyrolysis) شامل (250، 350، 450، 550، 650 و 750 درجه سانتی گراد) به کار رفت. سپس، از بیوچارهای به دست آمده به عنوان جاذب سدیم برای جذب این یون از یک آب شور که حاوی غلظت های مختلف NaCl بود استفاده شد. بعد از آن، مدل ایزوترم لانگمیر (LMM) و مدل ایزوترم Dubinin-Radushkevick (DRM) به کار رفت تا وابستگی سدیم جذب سطحی شده به غلظت سدیم در حالت تعادل به صورت کمی تعیین شود. تعیین کمی به روش LMM آشکار ساخت که با افزایش درجه حرارت، ظرفیت پیشینه بیوچارها برای جذب سطحی سدیم از مقدار 25/8 تا 67/8 میلی گرم در گرم زیاد شد. همچنین، مقدار EC کاهش یافت و مقدار K جابجا شده از روی بیوچار با افزایش درجه حرارت آتشکافت زیاد شد. تعیین کمی به روش DRM آشکار ساخت که سازوکار جذب سطحی سدیم عمدتاً یک فرایند فیزیکی است. نیز، رابطه ی معنادار بین مقدار سدیم جذب سطحی شده و مقدار K جابجا شده از بیوچار چنین اشاره داشت که سازوکار تبادل یونی میتواند هر دو حاضر باشد. خلاصه اینکه یافته های این پژوهش حاکی از آن است که می توان با استفاده از بیوچار و از طریق جذب سطحی فیزیکی، شوری آب لب شور را کاهش داد، EC را کم کرد، و نسبت K:N را افزایش داد.